

The flow alignment of some nematic liquid crystals

W. W. Beens and W. H. de Jeu

Solid State Physics Laboratory, University of Groningen, Melkweg 1, 9718 EP Groningen, The Netherlands

(Received 6 September 1984; accepted 11 October 1984)

A setup is described to determine the flow alignment angle θ_0 in nematic liquid crystals. Results for compounds with and without a strongly polar terminal cyano group indicate that the antiparallel dipole correlation associated with cyano groups has no influence on θ_0 . The influence of the occurrence of a smectic-A phase on θ_0 is investigated on three homologous series. The results show that θ_0 is a very sensitive probe for smectic-like short-range order. With increasing chain lengths a decrease of θ_0 is found, until finally no flow alignment exists anymore. Interestingly, a similar behavior is found in a homologous series without smectic phases.

I. INTRODUCTION

Nematic liquid crystals¹ are anisotropic liquids in which the constituting molecules are, on average, aligned with their unique axis parallel to a preferred direction in space. This direction is labeled by the director \mathbf{n} . Though a nematic liquid flows as easily as an isotropic liquid consisting of similar molecules, an analysis of the viscosities turns out to be rather complicated when the state of alignment, as given by \mathbf{n} , is considered. As to be expected, the flow depends on the angle between \mathbf{n} and the flow direction and the velocity gradient, leading to the three Miesowicz viscosities η_1 , η_2 , and η_3 (see, for instance, Ref. 2 or 3). However, in addition translational motions couple to inner orientational motions, and the flow will cause the director to rotate. This behavior can be described by the hydrodynamic theory of Ericksen⁴ and Leslie,⁵ which involves in total five independent viscosity coefficients.

It is the purpose of this paper to investigate in some detail for various compounds the relation between the flow and the orientation of \mathbf{n} . In the case of a simple two-dimensional shear flow (Fig. 1) and in the absence of external forces the torque density N working on \mathbf{n} is given by³

$$N = -(\kappa_1 \sin^2 \theta + \kappa_2 \cos^2 \theta)(\partial v / \partial x), \quad (1)$$

where κ_1 and κ_2 are the shear-torque coefficients that determine the torque on \mathbf{n} when it is parallel to the velocity gradient and the velocity \mathbf{v} , respectively, while θ is the angle between \mathbf{n} and \mathbf{v} . Equation (1) allows for an equilibrium value for which $N = 0$. This occurs for \mathbf{n} in the shear plane at the flow alignment angle θ_0 , determined by

$$\tan^2 \theta_0 = -\kappa_2 / \kappa_1. \quad (2)$$

A real solution for θ_0 requires the right-hand side of Eq. (2) to be positive. For many substances κ_2 turns out to be small negative. From thermodynamic reasons for rod-like molecules it is found that $\kappa_1 > 0$,² so that small values of θ_0 are expected. Interestingly in some substances κ_2 changes sign as a function of temperature, in which case no stable flow alignment exists anymore.⁶⁻¹¹

From the investigations to be presented it follows that any absence of flow alignment is not related to antiparallel dipole correlation of strongly polar molecules as has been suggested in the literature.^{6,12} In some homologous series the flow alignment angle only exists for the shorter members. The disappearance of θ_0 can be attributed to pretransitional smectic fluctuations,^{13,14} leading to a divergence of κ_2 . The flow alignment turns out to be an extremely sensitive measure for such effects, that can even be found if no smectic phase is actually observed.

In the next section first the experimental method and setup will be described. The results are given in Sec. III, while Sec. IV gives a concluding discussion. Some preliminary results have been given already in an earlier letter.¹⁵

II. EXPERIMENTAL

Following Gähwiler⁶ the flow alignment angle θ_0 is determined from the change in optical path difference between the ordinary and the extraordinary component of polarized light by comparing a situation with \mathbf{n} magnetically aligned along the flow direction and one without a magnetic field, respectively. For \mathbf{n} parallel to the z axis (see Fig. 1) the optical path difference Γ_0 will be

$$\Gamma_0 = (n_e - n_o)d, \quad (3)$$

n_o and n_e being the ordinary and extraordinary refractive indices, respectively, while d is the sample thickness. When \mathbf{n} makes an angle $\theta(x)$ with the z axis, the optical path difference Γ will be

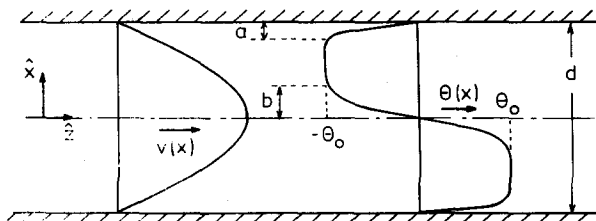


FIG. 1. Flow alignment in a flat capillary, with the velocity $v(x)$ and the angle $\theta(x)$.

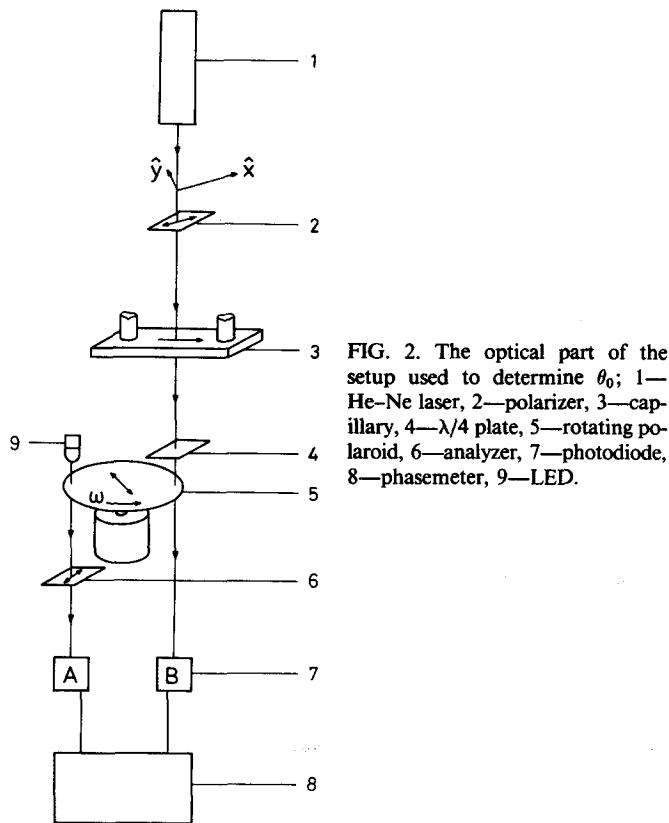


FIG. 2. The optical part of the setup used to determine θ_0 ; 1—He-Ne laser, 2—polarizer, 3—capillary, 4— $\lambda/4$ plate, 5—rotating polaroid, 6—analyzer, 7—photodiode, 8—phasemeter, 9—LED.

$$\Gamma = \int_{-d/2}^{d/2} [n(\theta) - n_o] dx, \quad (4)$$

with

$$\frac{1}{n^2(\theta)} = \frac{\sin^2 \theta}{n_o^2} + \frac{\cos^2 \theta}{n_e^2}. \quad (5)$$

In a situation of flow alignment $\theta(x)$ tends to the value θ_0 , except for thin transition layers at the boundaries and in the middle of the sample (see Fig. 1). In that situation $\theta(x)$ can be approximated by

$$\theta(x) = \begin{cases} -\theta_0, & x > 0, \\ \theta_0, & x < 0. \end{cases} \quad (6)$$

Using these results Eq. (4) reduces to

$$\Gamma = [n(\theta_0) - n_o]d. \quad (7)$$

The change in optical path difference upon removing the field is given by

$$\Delta\Gamma = \Gamma - \Gamma_0 = [n(\theta_0) - n_e]d. \quad (8)$$

With $\theta(x) = \theta_0$ Eqs. (5) and (8) can be combined and after some tedious rewriting one arrives at

$$\sin^2 \theta_0 = \frac{-2(\Delta\Gamma/n_e d) - (\Delta\Gamma/n_e d)^2}{[(n_e/n_o)^2 - 1][(\Delta\Gamma/n_e d) + 1]^2}. \quad (9)$$

$\Delta\Gamma$ can be determined experimentally from

$$\Delta\Gamma = \lambda\Delta\delta/2\pi, \quad (10)$$

where λ is the wavelength and $\Delta\delta$ is the change in the phase shift δ of the transmitted light between the situation of uniform \mathbf{n} (\mathbf{n} parallel to \mathbf{v} , using the external magnetic field) and the situation with \mathbf{n} at θ_0 with the flow direction \mathbf{v} (field switched off).

The phase shift δ between the ordinary and extraordinary component of the polarized light is determined with the setup shown in Fig. 2. The optical part of the setup is similar to the one used by Lim and Ho.¹⁶ The light beam from a He-Ne laser ($\lambda = 632.8$ nm) passes through a polarizer, the sample, a quarter-wave plate and a rotating polaroid before it reaches a photodiode. The polarizer is oriented at an angle of 45° with respect to the flow direction in the capillary. The quarter-wave plate is adjusted along the polarization of the incident light. This quarter-wave plate changes the elliptically polarized light from the sample back to plane-polarized light, but with the polarization direction rotated over an angle of $\delta/2$ with respect to the original direction. The light then passes through a rotating polaroid, that exists of a sheet of polaroid mounted on a cassette-recorder motor. The frequency ω can be changed between 1 and 35 Hz by varying the voltage. The light intensity I after the rotating polaroid is given by

$$I = 2I_0 \cos^2(\omega t + \delta/2) = I_0[1 + \cos(2\omega t + \delta)]. \quad (11)$$

The intensity of a reference beam, generated by a LED and passing through the rotating polaroid and an analyzer, is given by

$$I_{\text{ref}} = I_1[1 + \cos(2\omega t)]. \quad (12)$$

The relative phase difference between the two signals is measured with a sensitive phasemeter (Brüel and Kjær, type 2971).

The sample is placed in a high stability oven (Fig. 3). The rectangular capillary (Fig. 4) used is a modified

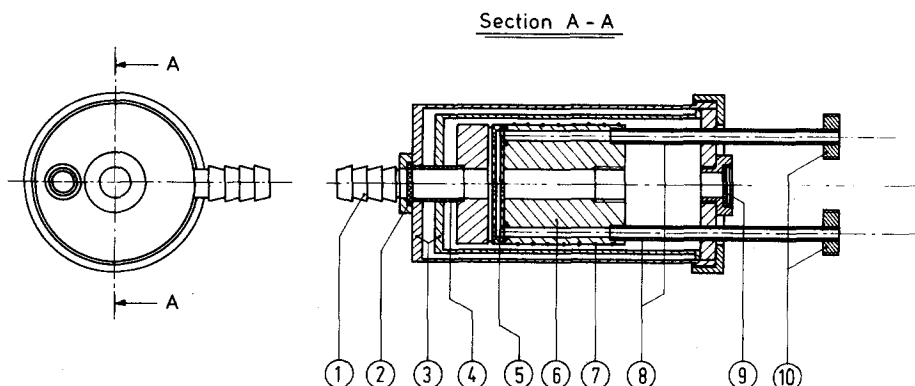


FIG. 3. Oven for flow alignment measurements; 1—connection for heating liquid, 2 and 9—glass windows, 3—hollow shield, 4 and 8—stainless steel tubes, 5—capillary, 6—copper cylinder, 7—heater, 10—connections to pressure difference system.

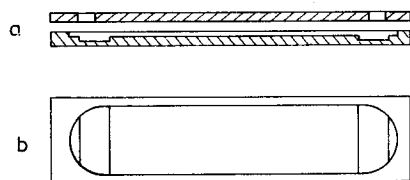


FIG. 4. (a) Side view of top and lower part of the rectangular capillary; (b) Top view of the lower part of the rectangular capillary.

version of a commercially obtainable flow capillary (Hellma Küvette 136-OS) with $d = 200 \mu\text{m}$. The capillary is pressed against a copper cylinder with two channels. A pressure difference of about 100 Pa is used to drive the liquid crystal from one channel inside the cylinder through the capillary into the other channel.

The oven has a two-stage heating system. The inner stage, consisting of the copper cylinder and the sample, is heated electrically. A thermistor, which is part of an ac-Wheatstone bridge, is used for the temperature setting. A second calibrated thermistor is used to determine the temperature. The second heating stage consists of a hollow shield, through which water or oil is circulated from a constant temperature bath. Usually, the shield is about 1° below the temperature of the sample. In this way it is possible to keep the sample temperature constant to better than 0.05°C .

The various compounds studied and their transition temperatures are given in Tables I and II.

III. RESULTS

In connection with the problems of the transition layers at the boundaries and in the middle of the sample first some measurements were done for N4 with $d = 200$ and $500 \mu\text{m}$, respectively. These results are given in Fig. 5 and agree well with each other.

In Fig. 6 results are given for two phenylbenzoates and two tolanes that differ in the presence or absence of a strongly polar end group, but are otherwise as similar as possible. The θ_0 values for each of the two pairs are very much the same.

Measurements have been performed on three different homologous series, for which the higher homologs have a smectic-A phase. For the *mAB* series (Fig. 7) starting with 7AB no flow alignment is found anymore. This is also the case for the highest measured homolog (CPE509) of the CPE50*m* series. The results for these series are shown in Fig. 8. Figure 9 gives the results for the *mCB* series.

Finally θ_0 has also been investigated for a homologous series without smectic phases. The results for these compounds, indicated as APAP*m*, are shown in Fig. 10. The trend in θ_0 with increasing chain length is very similar to that in the previous cases.

IV. DISCUSSION

In deriving Eqs. (7)–(9) the transition layers at the boundaries and in the middle of the sample were disregarded. In order to test this approximation experimentally,

let us discuss the case that $\theta(x) = 0$ at $x = \pm d/2$ (Fig. 1). The transition layers at the boundaries and in the middle have a thickness a and $2b$, respectively. Disregarding the transition layers is equivalent to assuming $\theta = \theta_0$ within these layers. The other limiting case is obtained by taking $\theta = 0$ within the layers. One then gets instead of Eq. (8)

TABLE I. Molecular structures of the compounds studied.

<i>mAB</i>	
	4,4'-di- <i>n</i> -alkylazoxybenzene
APAP <i>m</i>	
	Anisylidene-4-aminophenylacetate and higher homologues
<i>mCB</i>	
	4-alkyl-4'-cyanobiphenyl
CPE50 <i>m</i>	
	4-alkoxyphenyl- <i>trans</i> -4-pentylcyclohexylcarboxylate
CPEC	
	4-cyanophenyl- <i>trans</i> -4-pentylcyclohexylcarboxylate
N4	
	4- <i>n</i> -butyl-4'-methoxyazoxybenzene (mixture of both components)
7OT	
	4-heptyl-4'-methoxytolane
7CT	
	4-heptyl-4'-cyanotolane

TABLE II. Transition temperatures of liquid crystals studied (T_m = melting point, T_{AN} = smectic-A–nematic transition, T_c = clearing point).

Compound		T_m (°C)	T_{AN} (°C)	T_c (°C)
4AB	(DIBAB)	15.0	...	31.9
5AB	(PENTAB)	25.8	...	67.5
6AB	(HEXAB)	26.0	17.0	54.2
7AB	(HEBTAB)	34.2	53.9	70.6
APAPA1	(APAPA)	78.1	...	108.2
APAPA4		61.0	...	100.3
APAPA9		73.6	...	96.4
APAPA11		81.2	...	94.5
5CB		24.0	...	34.7
6CB		14.0	...	29.2
7CB		29.7	...	42.7
8CB		21.0	32.6	40.5
CPESO1		41.0	...	71.8
CPESO2		56.9	...	85.9
CPESO3		41.2	...	71.1
CPESO5		35.1	35.2	74.8
CPESO7		42.1	57.6	77.4
CPESO8		48.4	64.0	78.3–78.6
CPESO9		52.8	67.0	75.6
CPEC		47.6	...	79.5
N4		17.0	...	73.8
7OT		40.2	...	51.2–52.0
7CT		58.5	...	65.4–66.3

$$\Delta\Gamma = [n(\theta_0) - n_e][d - 2(a + b)]. \quad (13)$$

In reality θ varies over the distances a and b between the limits 0 and θ_0 , and $\Delta\Gamma$ will be given by

$$\Delta\Gamma = [n(\theta_0) - n_e][d - 2C(a + b)], \quad (14)$$

with $0 < C < 1$. From the results of Fig. 5 we note that the same θ_0 values are found for rather different values of d . This means that in Eq. (14) $2C(a + b) \ll d$, and that the assumption of taking $C \approx 0$ can be justified.

Molecules with a strongly polar CN group are well known to exhibit antiparallel dipole correlation.^{12,17} It has been suggested that this could influence the flow alignment, eventually leading to the disappearance of θ_0 .^{6,12} The results of Fig. 6 do not support this idea. In fact it excludes any important effect of antiparallel dipole association on the flow alignment.

From the results of the homologous series (Figs. 7–10) we note a trend of decreasing θ_0 with increasing chain

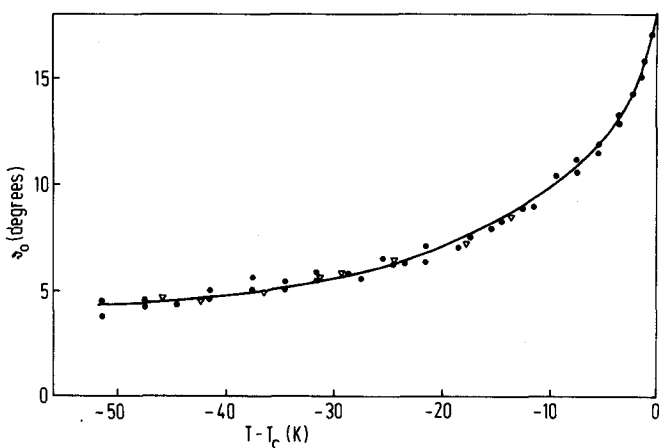


FIG. 5. Flow alignment angle θ_0 of N4; ● $d = 500 \mu\text{m}$, ▽ $d = 200 \mu\text{m}$.

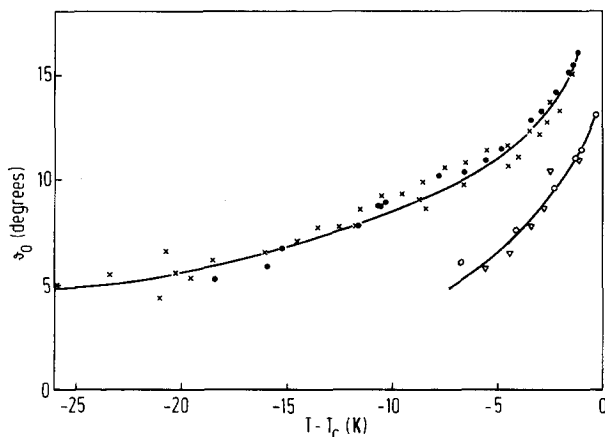


FIG. 6. Flow alignment angle θ_0 of CPEC (×); CPESO1 (●); 7OT (○) and 7CT (▽).

length, until finally the flow alignment disappears. Most of the compounds with this type of behavior possess a smectic-A phase. Therefore the possible influence of a smectic-A phase on the viscosities just above the smectic-A–nematic phase transition should be considered. McMillan¹³ and Jähnig and Brochard¹⁴ predicted an increase in $\gamma_1 = \kappa_1 + \kappa_2$ and in η_2 due to the fluctuations of the local smectic order parameter above a smectic-A–nematic phase transition. This can be understood in at least a qualitative way by considering a simple shear flow and including a smectic layer structure (Fig. 11).

In the case of \mathbf{n} parallel to the velocity gradient [η_1 and κ_1 , Fig. 11(a)] the flow direction is parallel to the smectic layers. As the layers can move with regard to each other, in a first approximation no influence of the smectic layer structure on η_1 and κ_1 is expected. The same applies to the situation of \mathbf{n} perpendicular to velocity and velocity gradient [η_3 , Fig. 11(b)] with again at most small changes of η_3 at the phase transition. For η_1 and η_3 this has been confirmed by measurements of Bhattacharya and Letcher.¹⁸ In the situation of \mathbf{n} parallel to \mathbf{v} [η_2 and κ_2 , Fig. 11(c)], the smectic layers are perpendicular to the flow direction. When there is flow the molecules have to move from one layer to another and must overcome the potential barrier associated with the layers. This leads to

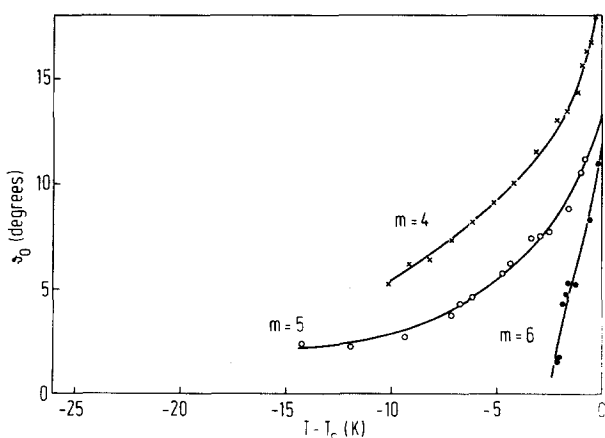
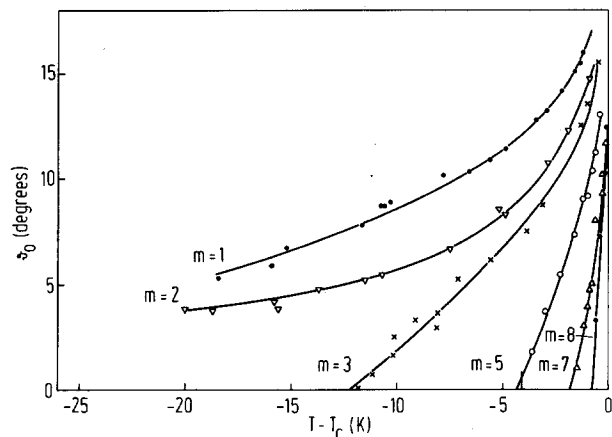
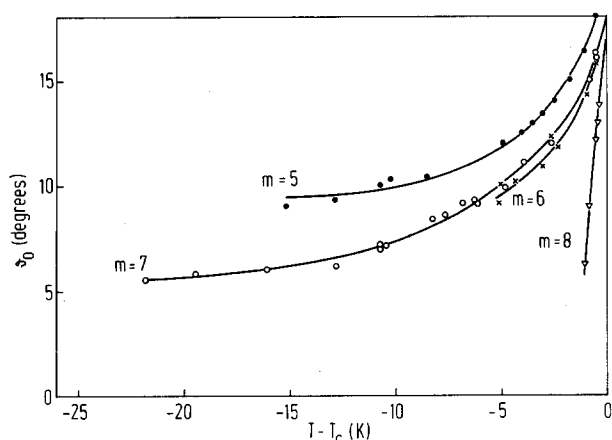
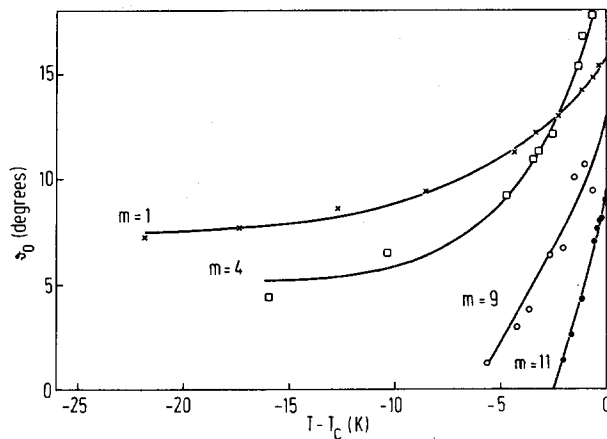


FIG. 7. Flow alignment angle θ_0 of the $m\text{AB}$ series.

FIG. 8. Flow alignment angle θ_0 of the CPESOm series.

increasing and finally diverging values for η_2 and κ_2 when the phase transition is approached. For η_2 this behavior has also been found experimentally by Bhattacharya and Letcher¹⁸ and by Knepe *et al.*¹⁹ As far as the rotational viscosities are concerned, direct measurements of κ_1 and κ_2 are not possible and we have to consider instead γ_1 and Eq. (2). The expected divergence of γ_1 near the smectic-A–nematic phase transition has been reported.^{20–23} From the above picture it follows that this must be due to the increase of κ_2 . As away from the phase transition $|\kappa_1| \gg |\kappa_2|$ there is a strong background for γ_1 that does not diverge. On the other hand θ_0 is more directly sensitive to these effects. As for rod-like nematogenic molecules κ_1 is necessarily positive,² a change of sign of $\tan^2\theta_0$ is due to a change of sign of κ_2 . If κ_2 increases due to presmectic fluctuations, it first changes sign from small negative values to positive ones and then diverges. This indicates that κ_2 and thus the flow alignment angle is extremely sensitive to pretransitional smectic effects. This makes the method suitable to detect the onset of presmectic fluctuations rather than the behavior close to the phase transition. In this way a presmectic increase of κ_2 might even be found without a smectic phase actually being observed. Most probably this is the reason for the disappearance of the flow alignment in CPES03 and some of the APAPA's. Believing that the experiments probe short-range smectic-like order, the

FIG. 9. Flow alignment angle θ_0 of the mCB series.FIG. 10. Flow alignment angle θ_0 of some APAPAm's.

question remains why in the APAPA series this does not lead to a long-range effect in the form of a phase transition to a smectic-A phase.

In principle one would like to correlate the variation of θ_0 with temperature and alkyl chain length with molecular properties of the system. In the literature several theories have been given that describe the flow alignment from a molecular point of view. However, taking a somewhat closer look, the final results of the various authors turn out to be rather similar. In our discussion so far the flow alignment angle θ_0 is determined by the ratio of the shear torques. In the derivation of the hydrodynamics of nematics given by Forster²⁴ $\lambda = 1/\cos 2\theta_0$ enters as an independent reactive coefficient. In the model

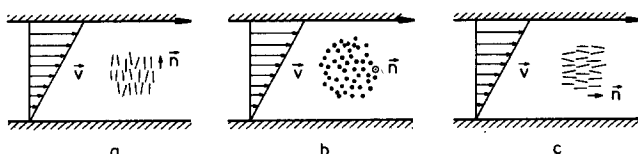
$$\cos 2\theta_0 = \frac{3S}{2\alpha + S}, \quad (15)$$

where

$$\alpha = \frac{I_l + 2I_t}{I_l - I_t}, \quad (16)$$

in which I_l and I_t are the moments of inertia of the molecules parallel and perpendicular to the long axis, respectively. For $\alpha = 1$, corresponding to the limit of infinitely long molecules, this expression reduces to results found by Marrucci²⁵ and by Doi.²⁶ In the case of ellipsoidal molecules $I_l/I_t = (W/L)^2$, where L is the length and W the width of the molecules, and this result has been derived earlier by Helfrich.^{27,28}

All these types of theory do not include any effect of presmectic fluctuations. As we have seen that θ_0 is extremely sensitive to such effects it is not surprising that the results from Eq. (15) are not in agreement with

FIG. 11. Possible shear flow for a smectic-A phase; a— η_1 and κ_1 , b— η_3 , c— η_2 and κ_2 .

experiments. In fact this is even true for the lower members of the homologous series and for N₄, in which cases presmectic effects can be expected to be least important.

ACKNOWLEDGMENTS

We wish to thank Dr. M. Clark (RRSE, Malvern, UK) for providing us with some of the higher homologs of the CPE50m series. We also wish to thank R. Postema for assisting with the measurements. This work forms part of the research program of the "Stichting voor Fundamenteel Onderzoek der Materie" (Foundation for Fundamental Research on Matter—FOM) and was made possible by financial support from the "Nederlandse Organisatie voor Zuiver Wetenschappelijk Onderzoek" (Netherlands Organization for the Advancement of Pure Research—ZWO).

¹ See, e.g., P. G. de Gennes, *The Physics of Liquid Crystals* (Clarendon, Oxford, 1974).

² F. M. Leslie, *Advances in Liquid Crystals*, edited by G. H. Brown (Academic, New York, 1979), Vol. 4, p. 1.

³ W. H. de Jeu, *Physical Properties of Liquid Crystalline Materials* (Gordon and Breach, New York, 1980).

⁴ J. L. Ericksen, *Mol. Cryst. Liq. Cryst.* **7**, 153 (1969).

⁵ F. M. Leslie, *Arch. Ration. Mech. Anal.* **28**, 265 (1968).

⁶ Ch. Gähwiller, *Phys. Rev. Lett.* **28**, 1554 (1972).

⁷ P. Pieranski and E. Guyon, *Phys. Rev. Lett.* **32**, 924 (1974).

⁸ P. E. Cladis and S. Torza, *Phys. Rev. Lett.* **35**, 1283 (1975).

⁹ M. G. Kim, S. Park, Sr. M. Cooper, and S. V. Letcher, *Mol. Cryst. Liq. Cryst.* **36**, 143 (1976).

¹⁰ K. Skarp, T. Carlsson, S. T. Lagerwall, and B. Stebler, *Mol. Cryst. Liq. Cryst.* **66**, 199 (1981).

¹¹ M. G. Clark, F. C. Saunders, I. A. Shanks, and F. M. Leslie, *Mol. Cryst. Liq. Cryst.* **70**, 195 (1981).

¹² W. H. de Jeu, *Philos. Trans. R. Soc. London Ser. A* **309**, 217 (1983).

¹³ W. L. McMillan, *Phys. Rev. A* **9**, 1720 (1974).

¹⁴ F. Jähnig and F. Brochard, *J. Phys.* **35**, 301 (1974).

¹⁵ W. W. Beens and W. H. de Jeu, *J. Phys. Lett.* **44**, L805 (1983).

¹⁶ K. C. Lim and T. J. Ho, *Mol. Cryst. Liq. Cryst.* **47**, 173 (1978).

¹⁷ A. J. Leadbetter, J. C. Frost, J. P. Gaughan, G. W. Gray, and M. Mosley, *J. Phys.* **40**, 375 (1979).

¹⁸ S. Bhattacharya and S. V. Letcher, *Phys. Rev. Lett.* **44**, 414 (1980).

¹⁹ H. Knepppe, F. Schneider, and N. K. Sharma, *Ber. Bunsenges. Phys. Chem.* **85**, 784 (1981).

²⁰ H. Knepppe, F. Schneider, and N. K. Sharma, *J. Chem. Phys.* **77**, 3203 (1982).

²¹ F. Hardouin, M. F. Achard, G. Sigaud, and H. Gasparoux, *Phys. Lett. A* **49**, 25 (1974).

²² F. Hardouin, M. F. Achard, and H. Gasparoux, *Solid State Commun.* **14**, 453 (1974).

²³ C. C. Huang, R. S. Pindak, P. J. Flanders, and T. J. Ho, *Phys. Rev. Lett.* **33**, 400 (1974).

²⁴ D. Forster, *Phys. Rev. Lett.* **32**, 1161 (1974).

²⁵ G. Marrucci, *Mol. Cryst. Liq. Cryst.* **72**, 153 (1982).

²⁶ M. Doi, *J. Polym. Sci. Polym. Phys. Ed.* **19**, 229 (1981).

²⁷ W. Helfrich, *J. Chem. Phys.* **50**, 100 (1969).

²⁸ W. Helfrich, *J. Chem. Phys.* **56**, 3187 (1972).